www.czasopisma.pan.pl PAN POLSKA AKADEMIA NAUK www.journals.pan.pl

A R C H I V E S O F M E T A L L U R G Y A N D M A T E R I A L S

Volume 58 2013 Issue 4

DOI: 10.2478/amm-2013-0184

D. BOCHENEK*, P. NIEMIEC*

TECHNOLOGY AND PROPERTIES OF FERROELECTROMAGNETIC LEAD-FREE BFN-FERRITE COMPOSITES

TECHNOLOGIA I WŁAŚCIWOŚCI FERROELEKTROMAGNETYCZNEGO BEZOŁOWIOWEGO KOMPOZYTU BFN-FERRYT

A lead free ceramic composite $0.9BaFe_{0.5}Nb_{0.5}O_3$-$0.1Ni_{0.5}Zn_{0.5}Fe_2O_4$ (BFN-NZF) with ferroelectromagnetic properties have been obtained in presented work. Ceramic composite powder obtained from the simple oxides Fe_2O_3, Nb_2O_5, ZnO, NiO and barium carbonate $BaCO_3$. The composition of the composite was chosen so that the ratio of the BFN and NZF components was 90:10. The synthesis of components of BFN-NZF composite was performed using the calcination method. Final densification of synthesized powder has been done using free sintering.

The XRD, the microstructure, EDS and dielectric investigations were performed. For comparison of the BFN ceramic and the BFN-NZF composites, temperature and frequency impedance research was conducted. Relaxation phenomena were observed at temperatures above 235°C in the BFN ceramic and above 150°C in the BFN-NZF composite. Obtained results show the coexistence of ferroelectric and magnetic properties. Such properties of obtained composites give the possibility to use them in magnetoelectric transducers.

Keywords: ferroelectromagnetic ceramic composites, multiferroics, smart materials, lead-free compounds

W niniejszej pracy otrzymano bezołowiowy ceramiczny kompozyt $0{,}9BaFe_{0.5}Nb_{0.5}O_3$-$0.1Ni_{0.5}Zn_{0.5}Fe_2O_4$ (BFN-NZF) o właściwościach ferroelektromagnetycznych. Ceramiczny proszek kompozytowy otrzymano na bazie prostych tlenków Fe_2O_3, Nb_2O_5, ZnO i NiO oraz węglanu baru $BaCO_3$. Skład kompozytu został dobrany w taki sposób, aby stosunek składników BFN i NZF wynosił 90:10. Syntezę składników kompozytu BFN-NZF przeprowadzono metodą kalcynacji proszków. Końcowe zagęszczanie syntetyzowanego proszku zostało przeprowadzone metodą spiekania swobodnego.

Zostały przeprowadzone badania XRD, mikrostrukturalne, EDS oraz właściwości dielektrycznych. Dla porównania ceramiki BFN i kompozytu BFN-NZF przeprowadzono temperaturowe i częstotliwościowe badania impedancyjne. Zjawiska relaksacyjne obserwowano w temperaturze powyżej 235°C w BFN ceramiki i powyżej 150°C w BFN-NZF kompozytu. Uzyskane rezultaty badań wskazują na współistnienie ferroelektrycznych i magnetycznych właściwości. Właściwości otrzymanych kompozytów dają możliwość wykorzystania ich do budowy przetworników magnetoelektrycznych.

1. Introduction

Multiferroics (smart materials) belong to the group of ferroic materials which exhibit simultaneously at least two kinds of physical states: ferromagnetic, ferroelectric, ferroelastic etc. [1-2]. Multiferroics have a much higher "intelligence" compared to ferroic materials, ie. react and respond to a more diverse spectrum of external factors (magnetic, electrical, mechanical, thermal, etc.) and offer more opportunities to be applied [1, 3-5]. They depend mainly on the degree of coupling of individual subsystems (magnetic, electric or elastic) [6].

Particularly important for practical applications of the compounds is the group of materials with a perovskite structure, containing lead in its composition. Properties of such materials, particularly in a ceramic form, to a large extent depend on the technological factors. Multicomponent ceramic materials belonging to the group of solid solutions of PZT ($PbZr_{1-x}Ti_xO_3$) are widely investigated in the world, due to great possibilities of practical applications of these materials [7]. Because of lead, the application of which is undesirable in the production of ceramics for environmental reasons, alternative lead-free materials with parameters comparable to ceramics lead are being sought. These include, for example: $BaTiO_3$, $SrTiO_3$, $BiFeO_3$, $Bi_{0.5}Na_{0.5}TiO_3$, $K_{0.5}Na_{0.5}NbO_3$, $Na_{0.5}Bi_{0.5}TiO_3$, $BaFe_{0.5}Nb_{0.5}O_3$, $Ba_{0.3}Na_{0.7}Ti_{0.3}Nb_{0.7}O_3$ [8-11].

Experimental work carried out so far in the optimization of technological process, modify compositions and applications of magnetic and ferroelectric materials, with a perovskite structure can be successfully used in the preparation, in experimental studies, and applications of multiferroic (ferroelectromagetic) ceramic composites of ferroelectric and magnetic properties.

In this paper, a two-component (lead-free) ceramic composite with ferroelectric and magnetic properties of powder-based ferroelectromagnetic $BaFe_{0.5}Nb_{0.5}O_3$ and ferromagnetic nickel-zinc ferrite, was obtained. The samples under-

* UNIVERSITY OF SILESIA, DEPARTMENT OF MATERIALS SCIENCE, ŚNIEŻNA 2, SOSNOWIEC, 41-200, POLAND

went X-ray, microstructure, impedance and dielectric properties examinations.

2. Experiment

Ceramic composite powder obtained from the simple oxides Fe_2O_3, Nb_2O_5, ZnO, NiO and barium carbonate $BaCO_3$ using classical technology. The appropriate quantities of reagents were weighed according to the formula $0.9BaFe_{0.5}Nb_{0.5}O_3+0.1Ni_{0.5}Zn_{0.5}Fe_2O_4$. The $BaFe_{0.5}Nb_{0.5}O_3$ (BFN) is the example of ferroelectric material, whereas the $Ni_{0.5}Zn_{0.5}Fe_2O_4$ (NZF) show features characteristic for a ferromagnetic one. The prepared reagents were mixed in a Fritsch-type planetary ball mill for 15 h (wet in ethanol). The technology of BFN ceramics fabrication is presented in detail in our previous paper [12].

Derivatographic analysis was performed on a Q-1500D derivatograph, (F. Paulik, J. Paulik, L. Erdey system) in order to select the optimal conditions for the synthesis of the composite powders (Fig. 1). On its basis, the following synthesis conditions were established: T_{synth} =1250°C, t_{synth} =2 h. Densification (sintering) of the composite powders was conducted at T_s =1350°C/t_s =4 h using the pressure-less sintering method. On the surfaces of composite samples (disk-shaped) electrodes were applied using silver paste burning method.

The X-ray tests were performed at room temperature on a diffractometer Philips X'pert (with a Cu lamp and a graphite monochromator) in the angular 2Θ from 12° to 62° (step 0.02° and measurement time 4 s/step). Microstructure, EDS (Energy Dispersive Spectrometry) and EPMA (Electron Probe Microbeam Analysis) tests were carried out using a scanning microscope HITACHI S-4700. Dielectric and impedance measurements were performed using QuadTech 1920 LCR meter for a cycle of heating (at frequencies of the measurement field from ν =0.02 kHz to 1.0 MHz).

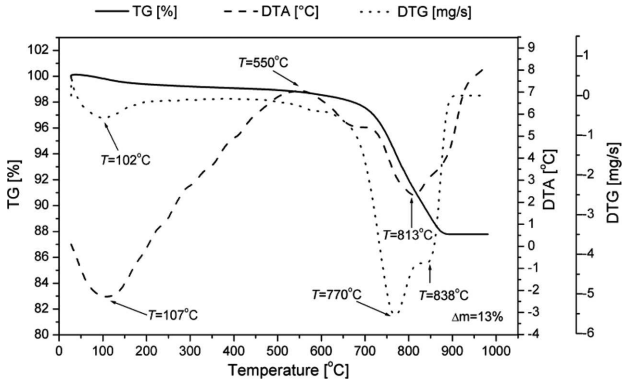

Fig. 1. DTA, TG and DTG curves of the BFN–NZF composite

3. Results and discussion

The X-ray analysis of the BFN-NZF composite revealed strong peaks originating from the $BaFe_{0.5}Nb_{0.5}O_3$ material and weak reflections from the $Ni_{0.5}Zn_{0.5}Fe_2O_4$ ferrite component (Fig. 2). The pattern shows that the BFN powder has monoclinic symmetry (with the best fit to the model 00-057-0771) [13], while the ferrite powder NZF shows a typical single phase cubic spinel. Composite samples are of low density (ρ =5.22 g/cm^3) and high porosity.

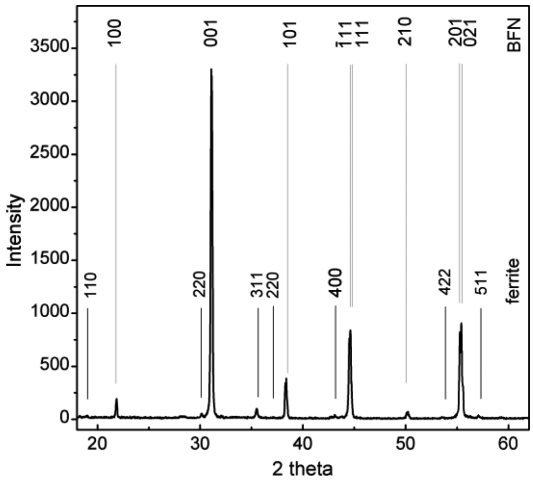

Fig. 2. XRD composite powder BFN-NZF

The X-ray EDS microanalysis was applied to investigate the homogeneity of composition, which consisted in scanning a specific micro-surface area of the sample and identification of individual elements in the spectrum of characteristic X-rays (qualitative and quantitative). The EDS analysis of the samples confirmed the expected composite percentage composition of various elements making up the compound (Fig. 3).

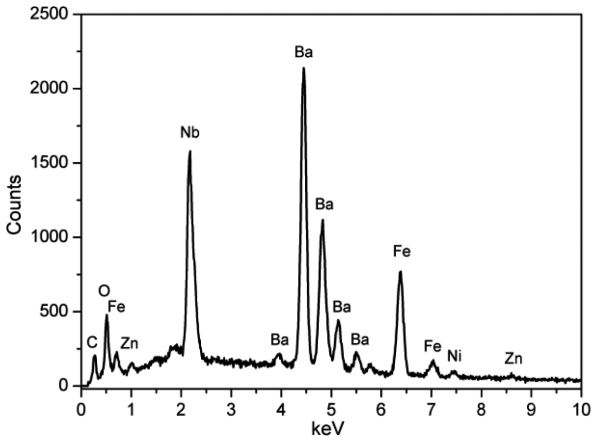

Fig. 3. EDS analysis for the BFN-NZF composite

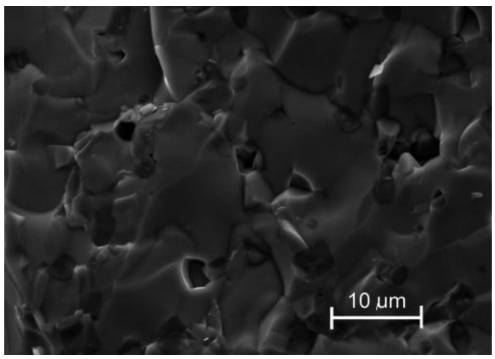

Fig. 4. SEM images of the fracture microstructure of the BFN-NZF composite

Fig. 4 presents SEM images of the fracture microstructure of the BFN-NZF composite samples. The BFN-NZF composite microstructure is characterized by bigger BFN grains surrounding the lower magnetic ferrite grains. An EPMA microanalysis was used to analyze the distribution of elements on the sample surface. The mappings obtained with the EPMA method with X-ray microprobe have confirmed a stoichiometry of analyzed compositions as well as the homogenous distributions of all elements throughout the whole volume of the samples (not presented in this work).

The ceramic composite of BFN-NZF has high values of electric permittivity (Fig. 5a). They may be associated with the formation of layers at a near-electrode surface (metal-semiconductor joint) that results from the sum capacity of the sample material and the capacity of the near-electrode formed layers. This near-electrode layer may be present in most of the materials with a perovskite-type structure, thereby increasing the value of dielectric permittivity. The described study was carried out by the authors of paper [14]. The $\varepsilon(T)$ dependence of the BFN-NZF composite also shows dispersive behavior (the so-called low-frequency dispersion). It results from the fact that as the frequency of the measuring field (ν) increases, the value of ε_m decreases (decrease maximum $\varepsilon_m(T_m)$), and the T_m temperature is shifted towards higher values.

As for the temperature dependency of the dielectric permittivity for the BFN-NZF composite, diffuse nature of the ferroelectric-paraelectric phase transition can be observed. Phase transition from the ferroelectric to paraelectric phase for the pure BFN ceramic occurs at about 245°C (for ν =1 kHz, heating cycle) [12] and in the BFN-NZF composite phase transition is at the same temperature (Fig. 5c). The value of the electric permittivity at the T_m of the BFN-NZF composite is much higher than pure BFN ceramic (for ν =1 kHz).

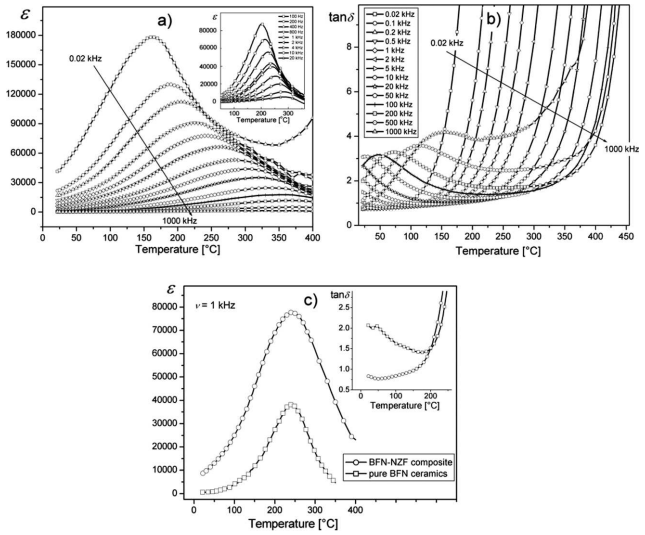

Fig. 5. Temperature dependencies of electric permittivity ε (a) and of the tangent of dielectric losses tanδ (b) of the BFN-NZF composite (heating). Inset Fig. 5a ε(T) for pure BFN ceramics. Comparison plots of the ε(T) and tanδ (T) for BFN-NZF composite and pure BFN ceramics, for ν =1 kHz (c)

In case the nickel-zinc ferrite the ferromagnetic-paramagnetic phase transition occurs at a temperature ⩾350°C. In the BFN-NZF composite increase diffusion of the phase transition of the electrical subsystem in compared to the pure BFN ceramics may be caused by overlapping phenomena associated with the electrical and magnetic properties (Fig. 5a and Fig. 5c). This may indicate the influence of the magnetic subsystem on the electrical properties. The value of dielectric loss for these materials is quite substantial and similar to the results presented in [15]. Their increase at higher temperatures is associated with increase the electrical conductivity (Fig. 5b). However, at lower temperature (from 20°C to 200°C) values of the tanδ for BFN-NZF composite are lower compared with pure BFN ceramics (Fig. 5c inset).

For the purpose of comparison of the BFN ceramic and the BFN–NZF composites, Figs. 6a and 6b show the variation of the real Z' and imaginary Z'' parts of impedance (respectively) as a function of frequency at different temperatures varying from 150°C to 350°C for the BFN ceramic, and Figs. 7a and 7b show the same graphs for the BFN-NZF composites. Inset this figures shown the magnification of Z' and Z'' (respectively) at high frequency range. As shown in Fig. 6a for BFN ceramic and Fig. 7a for BFN-NZF composites, it is observed that the magnitude of real Z' parts of impedance decreases with an increase in frequency and temperature.

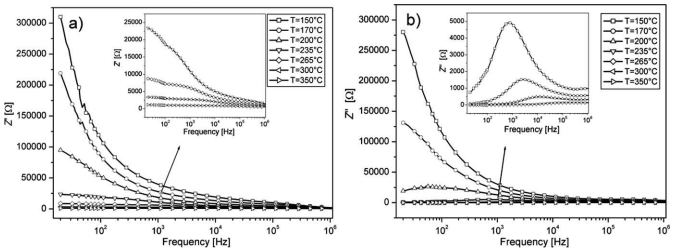

Fig. 6. Temperature and frequency dependent real (a) and imaginary (b) impedance spectra of BFN ceramics. Inset: high frequency range of which magnifies the peak positions (b)

For both compositions, Z'' decreases with increasing frequency and temperature (Fig. 6b and Fig. 7b). For the BFN ceramic (inset of Fig. 6b) at 235°C, a distinct peak appeared in Z'' at frequency of around 10^3 Hz. For BFN-NZF composites peak of the maximum appears above 10^2 Hz, but at lower temperature (150°C) (Fig. 7b). The values of imaginary Z'' parts of impedance were found to decrease with increasing temperature, indicating an increasing loss in the samples (increased conductivity). In the first and the second case, the Z'' peak became weaker in intensity and appeared to shift towards the high frequency side with increasing temperature. The next maxima become broader. This indicates that relaxation in these materials is a thermally activated process [16]. For both compositions, the merger of all the curves at high frequency indicates the depletion of space charges at those frequencies.

The occurrence of relaxation peaks in the imaginary part of the complex impedance in this frequency range might be due to the existence of the space-charge layer in the BFN-NZF composite sample. Space-charge polarization mechanism to predominate in heterogeneous structures, where a material is assumed to be composed of different areas (grain and grain boundaries). These phases have different electrical conductivity and thus accumulation of charges will be occurred at the

phase boundary [17]. These point charges result in an additional space charge polarization in the frequency range (10 Hz to 10^6 Hz), i.e. Maxwell-Wagner relaxation type (characteristic for heterogeneous dielectric materials) and it can by assume that the maximum is originated from the Maxwell-Wagner polarization between the BFN phase with higher resistivity and the NZF phase with much lower resistivity [17].

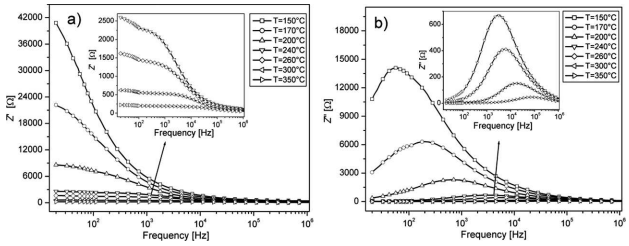

Fig. 7. Temperature and frequency dependent real (a) and imaginary (b) impedance spectra of BFN-NZF composite. Inset: high frequency range of which magnifies the peak positions (b)

For the BFN-NZF composites, this behavior also reflected the decreasing relaxation times (τ) calculated on the results in Fig. 7a according to the equation $\varpi\tau = 2\pi f_{max}\tau = 1$ [18]. The relaxation times τ decreases with increasing temperature (Fig. 8).

At higher temperatures, more electrons are thermally excited, so that the relaxation time of the carrier becomes the shorter and/or the dissipated thermal energy assists formed dipoles to follow the motion of the alternating field [19]. This result confirms the presence of temperature dependent electrical relaxation phenomena in the composite BFN-NZF. This variation of τ can be described by the known Arrhenius equation (1):

$$\tau = \tau_0 \exp\left(\frac{\Delta E_\tau}{k_B T}\right) \tag{1}$$

where: ΔE_τ – activation energy of the relaxation process, k_B – Boltzmann constant and τ_0 – characteristic relaxation time at infinite temperature. The plot of $\ln\tau$ v.1000/$T$for the composite BFN-NZF is shown in the inset of Fig. 8. The values of ΔE_τ and τ_0 were calculated from the intercept and slope of the linear fit and found to be 0.163 eV and 1.55×10^{-8} s, respectively.

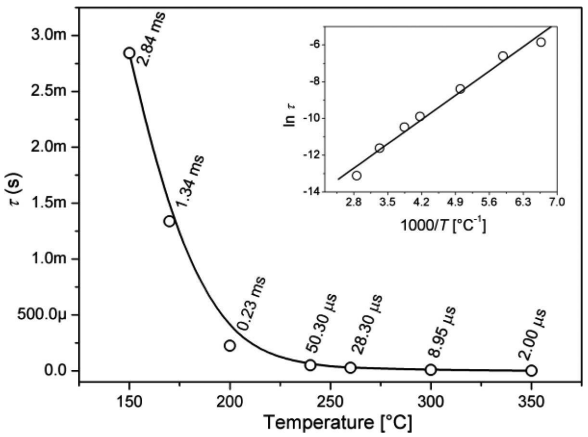

Fig. 8. Temperature dependence of the relaxation time (τ) for the BFN-NZF composite. Inset: $\ln\tau$ v.1000/T

4. Conclusion

The X-ray analysis of the $0.9BaFe_{0.5}Nb_{0.5}O_3$-$0.1Ni_{0.5}Zn_{0.5}Fe_2O_4$ (BFN-NZF) composite confirmed the presence of phases from the ferroelectric and magnetic component. Microstructure of the ferroelectro-ferromagnetic BFN-NZF composite consists of small grains of ferrite component surrounded by larger grains of the ferroelectric BFN component. The microstructural EPMA analysis showed that iron and other components of the composite are distributed throughout the volume of the sample uniformly.

Relaxation phenomena were observed at temperatures above 235°C in the BFN ceramic and above 150°C in the BFN-NZF composites. The occurrence of relaxation peak in the imaginary part of the complex impedance in this frequency range might be due to the existence of the space-charge layer in the BFN-NZF composite sample. It can by assume that the peak is originating from the Maxwell-Wagner polarization between the BFN phase with higher resistivity and the NZF phase with much lower resistivity (characteristic for two-phases ceramic composites with significantly different resistivity).

Comprehensive research of the ferroelectric-ferromagnetic composite showed the coexistence of ferroelectric and magnetic properties, which allows to use this type of composites for the construction of electromagnetic transducers.

Acknowledgements

We are grateful for the assistance of Anna Łatkiewicz (Laboratory of FE Scanning Microscopy and Microanalysis, Institute of Geological Sciences, Jagiellonian University, Krakow, Poland) for her help with the SEM pictures and XRD measurements.

REFERENCES

[1] D. Khomskii, Physics **2**, 20 (2009).
[2] D. Bochenek, Z. Surowiak, Phys. Status Solidi A **206**, 12, 2857-2865 (2009).
[3] D. Bochenek, P. Guzdek, J. Magn. Magn. Mater. **323**, 369-374 (2011).
[4] Z. Surowiak, D. Bochenek, Arch. Acoust. **33**, 2, 243-260 (2008).
[5] J.F. Scott, J. Mater. Chem. **22**, 4567-4574 (2012).
[6] K.F. Wang, J.-M. Liu, Z.F. Renc, Adv. Phys. **58**, 4, 321-448 (2009).
[7] R. Sitko, B. Zawisza, J. Jurczyk, D. Bochenek, M. Płońska, Microchim. Acta **144**, 9-15 (2004).
[8] C. Kruea-In, S. Eitssayeam, K. Pengpat, G. Rujijanagul, Mater. Res. Bull. **47**, 2859-2862 (2012).
[9] J.A. Bartkowska, J. Ilczuk, Int. J. Thermophys. **31**, 1-7 (2010).
[10] N.K. Singh, P. Kumar, R. Rai, J. Alloys Compd. **509**, 2957-2963 (2011).
[11] K. Ćwikiel, E. Nogas-Ćwikiel, Phase Transit. **80**, 1-2, 141-146 (2007).
[12] D. Bochenek, Z. Surowiak, J. Poltierova-Vejpravova, J. Alloys Compds. **487**, 572-576 (2009).
[13] S. Saha, T.P. Sinha, J. Phys.: Condens. Matter **14**, 249-258 (2002).
[14] K. Wójcik, K. Zieleniec, M. Mulata, Ferroelectrics **289**, 107-120 (2003).

[15] S. Eitssayeam, U. Intatha, K. Pengpat, T. Tunkasiri, Curr. Appl. Phys. **6**, 316-318 (2006).
[16] K. Prabakar, S.P. Mallikarjun Rao, J. Alloys Compd. **437**, 302-310 (2007).
[17] H. Zhang, M. Chee-Leung, J. Alloys Compd. **513**, 165-171 (2012).
[18] D. Bochenek, P. Niemiec, A. Chrobak, G. Ziółkowski, A. Błachowski, Mater. Charact. (2013), doi: 10.1016/j.matchar.2013.10.027
[19] I.S. Yahia, M. Fadel, G.B. Sakr, S.S. Shenouda, F. Yakuphanoglu, W.A. Farooq, Acta Phys. Pol. A **120**, 3, 563-566 (2011).

Received: 20 September 2013.